applied sciences

MDPI

Article

A Masterpiece from the Renaissance: The *Offiziolo di Durazzo*

Elisa Calà [1], Angelo Agostino [2], Cristina Fornacelli [3], Marcello Picollo [3], Emanuela Ferro [4] and Maurizio Aceto [1,*]

[1] Dipartimento per lo Sviluppo Sostenibile e la Transizione Ecologica, Università degli Studi del Piemonte Orientale, Piazza S. Eusebio, 5-13100 Vercelli, Italy; elisa.cala@uniupo.it
[2] Dipartimento di Chimica, Università degli Studi di Torino, Via P. Giuria, 7-10125 Torino, Italy; angelo.agostino@unito.it
[3] Istituto di Fisica Applicata "Nello Carrara" del Consiglio Nazionale delle Ricerche (IFAC-CNR), Via Madonna del Piano, 10-50019 Sesto Fiorentino, Italy; c.fornacelli@ifac.cnr.it (C.F.); m.picollo@ifac.cnr.it (M.P.)
[4] Sezione di Conservazione, Biblioteca Civica Berio, Via del Seminario, 16-16121 Genova, Italy; eferro@comune.genova.it
* Correspondence: maurizio.aceto@uniupo.it

Featured Application

The characterisation of the materials with which the manuscript was composed and decorated is strategical from the point of view of conservation, to plan the proper conditions for storage and for exposition in cases when it is requested for exhibition.

Abstract

The manuscript known as *Offiziolo di Durazzo*, a Book of Hours kept in Genoa at Biblioteca Civica Berio, is among the most notable artistic evidence of the Renaissance. The manuscript was investigated through a fully non-invasive approach involving UV–visible fibre-optic diffuse reflectance spectrophotometry (FORS), X-ray fluorescence spectrometry (XRF), multiband imaging (MBI), and hyperspectral imaging (HSI). The study focused on both the purple parchment and the decorative apparatus, with the aim of improving our understanding of the materials, manufacturing techniques, and state of conservation, while providing scientific evidence to support appropriate conservation strategies, including storage and exhibition conditions. The results of the spectroscopic investigation represent the consistent characterisation of the palette used by the artist Francesco Marmitta, revealing a rich and heterogeneous selection of valuable materials, such as ultramarine blue, vermillion, insect dyes, malachite, gold, and silver. MBI and HSI enabled a spatial investigation of the materials and colour across the manuscript. HSI data were used for both material mapping and colour analysis, revealing subtle spatial heterogeneities associated with the parchment structure, dye distribution, and conservation-related phenomena. HSI data were further exploited to obtain CIELAB colour maps, enabling the assessment of chromatic variability across the manuscript. In decorated areas, the combined interpretation of MBI and HSI spectral mapping allowed the visualisation of the colourant distribution and paint mixtures, providing insights into artistic techniques, material selection, and workshop practices.

Keywords: non-invasive; orchil; FORS; XRF; MSI; manuscript; purple; parchment

Academic Editors: Amélia Dionísio and Graça Vasconcelos

Received: 11 June 2026
Revised: 2 July 2026
Accepted: 10 July 2026
Published: 14 July 2026

1. Introduction

The *Durazzo Book of Hours*, or *Offiziolo di Durazzo*, likely created in Parma in the early 16th century, is a luxurious prayer book, characterised by purple parchment and chrysography, or gold lettering [1]. The term *offiziolo* means "little office", denoting a devotional book intended for private prayer, in contrast to the "great office" reserved for the clergy. The combination of a golden ink on a purple writing support recalls the tradition of the purple codices, i.e., the biblical manuscripts produced from the Roman age to the Carolingian and Byzantine periods, which were addressed to an elite clientele, reflecting the long-standing association of purple with imperial authority, prestige, and social distinction.

With six full-page miniatures, 15 smaller ones, a series of months, and over 200 figured initials among its 219 folios, the codex is considered the finest work of the Parma-born miniaturist and painter Francesco Marmitta, also the author of the *San Quintino Altarpiece*, now in the Louvre. Three collaborators are present in minor artistic features. The incredibly accurate and clean drafting of the text in chrysography is attributed to the Emilian calligrapher Pietro Antonio Sallando.

The chiselled friezes on the binding echo the interior decorations, so closely resembling one another that it suggests the intervention of the same miniaturist (or, more likely, one of his associates). The unmistakable binding led to the recognition of the *Offiziolo di Durazzo* in the small book displayed by an unidentified figure portrayed in the painting *Portrait of a Collector* by Parmigianino, now in the National Gallery in London and dated 1523–24. It can be deduced that, during these years, the codex was in Parma, where Marmitta had returned at the end of his career, before dying in 1505 during a plague epidemic.

No further documentary evidence concerning the *Offiziolo di Durazzo* is known regarding the period prior to 1826, when it reappeared in Genoa in an inventory of assets bequeathed by the merchant Antonio Bacigalupo, a Genoese man with a Portuguese mother. His widow sold it to the Marquis Marcello Luigi Durazzo, a refined art connoisseur, who, in 1847, bequeathed it to the Biblioteca Civica Berio in Genoa, where it is kept now as ms. Arm. 1. The patron of the codex remains unknown, and, for this reason, it has taken the name of its last owner.

At the outbreak of World War II, the office shared the fate of other "precious relics" owned by the city, including Columbus's autographed letters and Paganini's violin, and was transported to places considered safe. Returning to Genoa, they were placed in the City Hall's air-raid shelter in a zinc box built into a recess, with holes to promote air circulation and reduce humidity. Thanks to these measures, the *Offiziolo di Durazzo* has survived intact to the present day [2].

Since 1998, the manuscript has been housed on the new premises of the Biblioteca Berio in Genoa, within a climate-controlled repository dedicated to parchment materials and featuring a constant temperature and humidity; it is kept inside a custom-made display case regulated by silica gel and fitted with protective glass. Thanks to this new case, designed to serve both preservation and display functions and created alongside the publication of the facsimile in Franco Cosimo Panini's "La Biblioteca Impossibile" series, the *Offiziolo di Durazzo* was exceptionally put on public display in 2023 during the autumn edition of the "Rolli Days" event (13–15 October). This event marked the opening of the bicentennial celebrations of the civic library, coinciding with the year that Genoa served as the Italian Capital of Books. The facsimile can be appreciated at the following website: https://replica.francopanini.it/opera/libro-dore-durazzo (accessed on 1 July 2026).

As part of the PURPLE project titled Purple Parchment Legacy: Art History and Heritage Science for the Study of Manuscript Painting from Late Antiquity to the Modern Age (5th–19th centuries), funded by PRIN 2020, the *Offiziolo di Durazzo* has been the subject of an in-depth, yet completely non-invasive, diagnostic campaign aimed at uncovering the secrets of its production and clarifying its state of health. The study has been conducted using both specific spectroscopic techniques, such as UV–visible fibre-optic diffuse reflectance spectrophotometry (FORS), X-ray fluorescence spectrometry (XRF), and optical microscopy, and multiband and hyperspectral imaging (HSI) techniques. All analyses have been carried out on the premises of the Biblioteca Civica Berio to minimise stress caused to the manuscript (example in Figure 1).

Figure 1. FORS analysis of the *Offiziolo di Durazzo*.

2. Materials and Methods

2.1. UV–Visible Diffuse Reflectance Spectrophotometry with Optic Fibres (FORS)

The FORS analysis was performed with an Avantes (Apeldoorn, The Netherlands) AvaSpec-ULS2048XL-USB2 model spectrophotometer and an AvaLight-HAL-S-IND tungsten halogen light source; the detector and light source were connected with fibre-optic cables to an FCR-7UV200-2-1,5 $\times$ 100 probe. In this configuration, both the incident and detecting angles were 45° from the surface normal in order not to include specular reflectance. The investigated area on the sample had a 1 mm diameter. The probe was held by hand in contact with the sample, and the tip of the probe was covered with a small cylindrical sheath, properly cut to fit the measurement angle, in order to exclude external sources of light. The spectral range of the detector was 200–1160 nm; the overall operational range of the device (combination of lamp + detector) was 375–1100 nm. Depending on the features of the monochromator (slit width 50 μm, grating of UA type with 300 lines/mm) and of the detector (2048 pixels), the best spectral resolution was 2.4 nm, calculated as the FWHM. Diffuse reflectance spectra of the samples were referenced against the WS-2 reference tile provided by Avantes and guaranteed to be reflective at 98% or more in the spectral range investigated. The instrumental parameters were as follows: 10 ms integration time; 100 scans for a total acquisition time of 1.0 s for each spectrum. The whole system was managed by means of the AvaSoft v. 8 dedicated software, running under Windows 11^{TM}.

2.2. X-Ray Fluorescence Spectrometry (XRF)

XRF measurements were performed with an EDXRF Thermo (Waltham, MA, USA) NITON spectrometer XL3T-900 GOLDD model, equipped with an Ag tube (max. 50 kV, 100 μA, 2 W) and a large-area silicon drift detector (SDD), with an energy resolution of about 136 eV at 5.9 keV. The analysed spot had an average diameter of 3 mm and was focused by a CCD camera with a working distance of 2 mm. Measurements were performed using two different processing algorithms. The "Metal" algorithm, employed for the analysis of noble metal binding and the golden inks, consisted of three operating conditions: main (40 keV, 50 μA, Fe/Al filter), low (20 keV, 95 μA, Cu filter), and light (6 keV, 95 μA, no filter). For the analysis of the colourants in the miniatures and the gemstones in the binding, the "Mining" algorithm was used, comprising four operating conditions: high (50 keV, 50 μA, Mo filter), main (40 keV, 50 μA, Fe/Al filter), low (20 keV, 95 μA, Cu filter), and light (6 keV, 95 μA, no filter). Each operating condition was applied for 30 s, during which the instrumental parameters were automatically adjusted to optimise the analytical response over the different energy ranges. The total time of analysis, therefore, was 90 s in the "Metal" mode and 120 s in the "Mining" mode The instrument was held in position with a moving stage allowing millimetric shifts in order to reach the desired probe-to-sample distance; the stage was laid on a tripod. The obtained spectra were processed with the commercial software BAxil v. 1.1 (Brightspec NV/SA, Niel, Belgium), derived from the academic software QXAS from IAEA.

2.3. Optical Microscopy

A USB Dino-Lite (New Taipei City, Taiwan) AM4113T-FV2W model microscope was used to acquire digital images at 50× and 200× magnification ratios. The instrument is equipped with 375 nm and visible LED lights and a digital camera with a 1.3-megapixel resolution.

2.4. Multiband Imaging

A modified digital imaging system based on a Canon EOS RP mirrorless camera equipped with a 26.2-megapixel full-frame silicon CMOS sensor coupled with an EF 50 mm f/1.8 STM lens was used for MBI investigations. The camera was modified to extend its spectral sensitivity over the 360–1100 nm range.

Visible (Vis) and infrared (IR) acquisitions were carried out using two 50 W HALOSTAR ST (ams-OSRAM AG, Premstaetten, Austria) 12 V low-voltage tungsten halogen lamps characterised by a correlated colour temperature of approximately 2950 K and a colour rendering index (CRI) of Ra = 100, selected for their broad and continuous spectral emission across the visible and near-infrared regions. Ultraviolet-induced visible luminescence (UVL) imaging was instead performed using two CTS ART LUX 100LW LED (CTS, Altavilla Vicentina, Italy) sources modified at IFAC-CNR through the integration of a UG11 filter to suppress residual visible emission and improve the excitation spectral purity.

Visible imaging acquisitions were performed using a Kolari Vision UV/IR Cut Hot Mirror Pro 2 filter to restore the spectral response of the modified camera by compensating for the removal of the original internal infrared-blocking filter. During UVL imaging, an additional UV 422 nm filter (50 × 50 mm, Asahi Spectra, Torrance, CA, USA) was also mounted to suppress reflected ultraviolet radiation and selectively record luminescence emission from the investigated surface. A long-pass 850 SCF-50S-85IR BLlck filter (OptoSigma® Europe, Les Ulis, France), characterised by a cut-on wavelength of 850 nm, was used during IR acquisitions.

2.5. Hyperspectral Imaging

Hyperspectral imaging (HSI) data were acquired using a portable push-broom hyperspectral imaging system (Specim® IQ, Spectral Imaging Ltd., Oulu, Finland), operating in the 400–1000 nm spectral range. The instrument provides 204 spectral bands with a mean spectral resolution of approximately 7 nm and a spectral sampling interval of 3.5 nm. The system integrates a hyperspectral camera, an internal scanning mirror, embedded processing electronics, and a touchscreen interface within a compact module (207 × 91 × 74 mm; 1.3 kg). Each acquisition generates a hyperspectral cube consisting of two spatial dimensions (512 × 512 pixels) and one spectral dimension (204 bands), providing a full reflectance spectrum for every pixel within the imaged area.

Prior to each acquisition session, calibration was performed using a 99% reflectance Spectralon® reference standard according to two manufacturer-defined white referencing procedures. Dark current correction was automatically applied through the instrument's internal shutter.

All measurements were carried out in a darkened environment to minimise interference from ambient illumination. Illumination was provided by two 50 W low-voltage tungsten halogen lamps (HALOSTAR ST, 12 V), characterised by a correlated colour temperature of approximately 2950 K and a colour rendering index (CRI) of Ra = 100. The lamps were equipped with ultraviolet filtering elements to minimise potentially harmful UV emission.

A dual-source 45°/0° illumination–observation geometry (2 × 45°/0°) was adopted to ensure homogeneous illumination across the manuscript surface while minimising specular reflection effects.

The exposure conditions were carefully optimised to ensure minimal light exposure and thermal impact in order to prevent any risk of damage to the parchment during measurements [3]. The manuscript was kept covered between successive acquisitions and exposed only for the time strictly required for the acquisition of each individual folio (typically less than 90 s).

Hyperspectral datacubes were processed following two complementary workflows dedicated to material mapping and colour analysis, respectively [4,5]. Reflectance spectra were extracted after calibration using the white reference acquired during image acquisition. Spectral similarity analysis based on the Spectral Angle Mapper (SAM) algorithm [6] implemented in Specim IQ Studio v. 1.0 was then applied to generate spatial maps of spectrally similar materials. Representative endmember spectra were selected from homogeneous regions identified on the HSI images and supported by the FORS analyses. Similarity thresholds (typically >0.995) were empirically adjusted for each endmember to maximise discrimination between spectrally similar paint layers while minimising isolated misclassified pixels.

The spectral information was exploited to identify and map pigments and colourants, while the corresponding CIELAB coordinates were used to characterise the colour of the purple parchment and assess its spatial variability.

Reflectance data were converted into CIELAB coordinates to obtain spatially resolved colorimetric maps (L*, a*, and b*) and differential chromatic maps (Δa* and Δb*), which were used to investigate the colour distribution and visualise localised chromatic alterations of the purple parchment.

Colorimetric Processing of Hyperspectral Data

Reflectance spectra extracted from the hyperspectral datacubes (400–1000 nm) were interpolated from the native 3.5 nm spectral sampling interval to a 1 nm interval using the interp1d function implemented in the SciPy library (version 1.17.0, https://docs.scipy.org/doc/scipy-1.17.0/reference/generated/scipy.interpolate.interp1d.html (accessed on 1 July 2026), applying cubic interpolation. The interpolated reflectance spectra were then converted into CIELAB colour coordinates according to the CIE recommendations for the D65 illuminant and the 2° Standard Observer [7–9]. The resulting L*, a*, and b* values were calculated for each image pixel, generating spatially resolved grayscale TIFF images corresponding to the three colour coordinates [10]. Regions of interest (ROIs) were selected to extract colorimetric values from representative homogeneous areas, avoiding edges, damaged regions, and zones with strong textural variations. An ROI size of 15 × 15 pixels was selected to ensure an adequate spatial resolution while minimising the influence of local signal fluctuations and small-scale variability related to surface inhomogeneities.

To enable direct comparison between different folios, all HSI-derived colour maps corresponding to the same colour coordinate (L*, a*, b*) were displayed using fixed colour lookup tables (LUTs). Fixed display ranges were defined from the minimum and maximum values measured in representative ROIs selected from well-preserved parchment areas. The same LUTs and display limits were applied to all folios. This approach enabled a direct comparison among folios while avoiding visual biases introduced by the automatic contrast stretching applied independently to each image. LUTs were used to enhance subtle spatial variations, without altering the underlying colour values.

To facilitate the visualisation of localised colour alterations, differential chromatic maps were generated by comparing the colour coordinates of each pixel with reference values representative of the well-preserved purple parchment. The reference coordinates were calculated from well-preserved areas distributed throughout the manuscript. Differential maps were then calculated according to

$$\Delta a^* = a^*_{pixel} - a^*_{ref}$$

$$\Delta b^* = b^*_{pixel} - b^*_{ref}$$

where a^*_{pixel} and b^*_{pixel} are the colour coordinates of each pixel, and a^*_{ref} and b^*_{ref} are the average reference values. Positive and negative values therefore represent local chromatic deviations from the reference condition and enable the visualisation of subtle colour changes across the parchment surface. LUTs and display ranges for the differential maps (Δa* and Δb*) were defined using the lower and upper percentiles of the global distribution of differential values. This approach minimises the influence of isolated outliers while preserving direct comparability between folios and enhancing the visualisation of subtle chromatic deviations associated with colour alteration.

3. Results

The complementary use of spectroscopic techniques (FORS and XRF) and imaging (MBI and HSI) methods provides a comprehensive and non-invasive approach to investigating both material characteristics and conservation issues in historical manuscripts [5,11–13]. The conventional, point-based techniques yield information about the molecular and elemental compositions of the materials studied [14,15]. By investigating differences in spectral response across the ultraviolet (UV), visible (Vis), and near-infrared (NIR) regions, MBI and HSI can enhance features that are difficult to discern under conventional observation [16–19]. Imaging analytical techniques may also contribute to investigating several technological aspects of manuscript production and conservation.

The results supported a better understanding of both the material composition and the conservation history of the *Offiziolo di Durazzo*, demonstrating the diagnostic potential of non-invasive imaging approaches for studying historical, purple-dyed parchments.

The following sections present the results of the non-invasive diagnostic campaign, focusing on different key components of particular interest from both an artistic and technological perspective, including the purple-dyed parchment support, the extensive use of golden ink, the rich decorative apparatus, and the binding created with gold and silver.

3.1. The Purple Parchment

The most relevant feature of the *Offiziolo di Durazzo* is its purple parchment—evidence of the patron's power, given the symbolic meaning of the purple colour. The deep hue of the parchment was obtained by applying a solution of orchil—a dye extracted from several species of lichen upon fermentation in ammonia. The identification of orchil was achieved by means of FORS, with the typical absorption bands at ca. 545 and 590 nm [20], together with the typical shape of the spectrum (Figure 2).

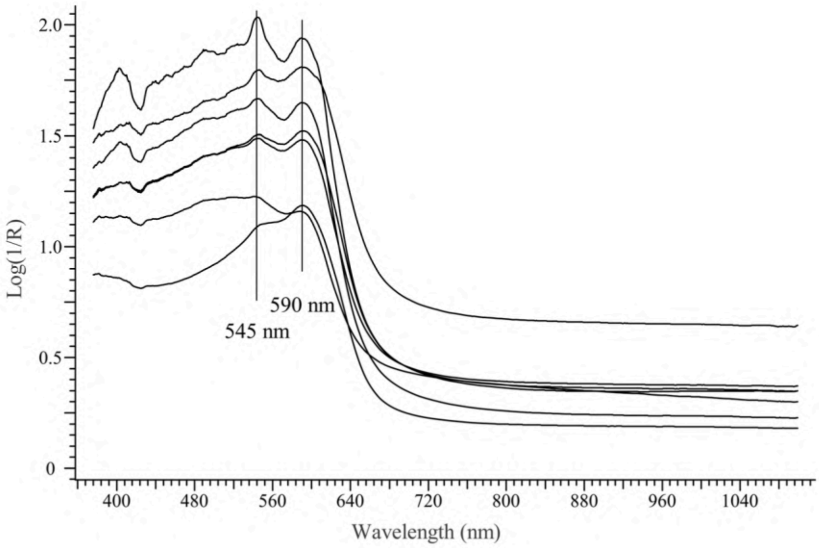

Figure 2. FORS spectra in Log(1/R) coordinates of the purple parchment, taken from different folios.

The purple colouration is highly consistent throughout the manuscript, and no signs of rubbing or brushing can be observed. This suggests that the parchment was most likely dyed by soaking in a dye bath, rather than by the application of a colouring solution onto the surface. Such a process, similar to textile dyeing, would account for the uniform distribution of the colourant and contrasts with the brushing or painting procedures typical of Late Antique and early medieval traditions [21].

Among the investigated techniques, UVL proved particularly effective in visualising subtle spatial variability within the parchment–dye system. The technique enhanced local differences in optical response that may reflect variations in dye distribution, dye–substrate interaction, or support-related properties not readily detectable under visible illumination. Most of the examined folios exhibited a relatively homogeneous luminescence response, indicating generally uniform optical behaviour throughout the manuscript. Representative examples are shown in ff. 8r and 68r (Figure 3a,b, respectively), where the parchment displays a continuous optical response with only limited small-scale variability and no evident large-scale luminescent domains. Slight local variations were detectable, but these appeared distributed at a small spatial scale and did not produce structured heterogeneity.

UVL imaging also revealed structural features associated with the parchment substrate itself. In particular, elongated darker domains, diffuse cloud-like features, and fine linear structures become visible across the parchment surface. These patterns are especially evident in f. 9r (Figure 3c), where a network of narrow elongated features and irregular domains can be distinguished throughout the support. On the other hand, f. 144r (Figure 3d) reveals a diffuse pattern distributed across the entire parchment surface. The morphology and spatial distribution of these features suggest a correlation with the natural heterogeneity inherited from the original animal dermis, including local variations in collagen organisation, fibre density, porosity, and residual anatomical structures [22].

(**a**) (**b**) (**c**) (**d**)

Figure 3. UVL images of selected folios from the Durazzo Book of Hours. (**a**,**b**) Representative examples of folios exhibiting a relatively homogeneous luminescence response (ff. 8r and 68r), where the generally uniform optical behaviour of the purple-dyed parchment can be observed. (**c**) f. 9r, showing elongated darker features and irregular domains distributed across the support. (**d**) f. 144r, an example of a diffuse mottled pattern extending over the parchment surface, consistent with natural heterogeneities in the parchment substrate.

Although the overall appearance of the manuscript was found to be homogeneous, localised luminescence heterogeneity was observed in several folios (such as ff. 5r, 13r, and 168r). Representative examples are reported in Figure 4, where brighter and darker domains are distributed across the purple support. Meanwhile, f. 5r (Figure 4a) is characterised by a diffuse cloud-like pattern extending over most of the folio, whereas f. 13r (Figure 4b) shows more localised, elongated domains with a preferential orientation. In f. 119r (Figure 4c), subtle differences between the central text panel and the surrounding border can also be observed, where the outer frame shows a more structured texture and enhanced local heterogeneity relative to the central writing area.

(**a**) (**b**) (**c**)

Figure 4. *Cont.*

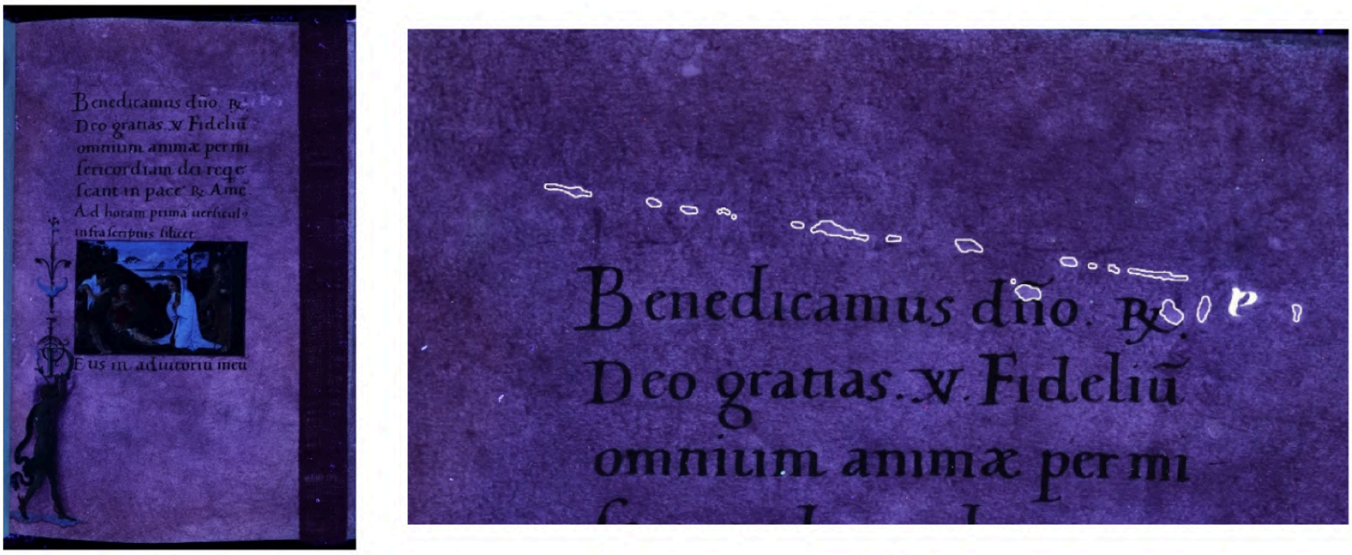

(**d**) (**e**)

Figure 4. Ultraviolet-induced visible luminescence (UVL) images showing examples of localised luminescence heterogeneity observed in selected folios of the Durazzo Book of Hours. (**a**) f. 5r, characterised by a diffuse cloud-like pattern distributed across the surface. (**b**) f. 13r, showing elongated luminescent domains on the bottom-right corner, characterised by a preferential orientation. (**c**) Detail at f. 119r, where subtle differences can be observed between the central text panel and the surrounding border. (**d**,**e**) f. 58r, a discontinuous feature crossing the upper portion of the writing area and partially overlapping the text. The morphology of this anomaly is compatible with transferred graphic material and appears unrelated to the general distribution of the purple dye.

Finally, peculiar, localised anomalies unrelated to the general distribution of the purple dye can be observed in f. 58r (Figure 4d,e). Here, a discontinuous luminescent feature extends across the upper portion of the writing area, locally overlapping the text and displaying shapes compatible with transferred graphic material.

3.2. The Golden Text

The text was written by the Italian scribe Pietro Antonio Sallando, born in Reggio Emilia, a teacher of grammar and calligraphy at Università di Bologna. He was described as "*Il più excellente scriptore credo habia il mondo per la varietà delle littere*" ("the most excellent writer that I believe the world has for the variety of letters") in a letter from the writer Giovanni Sabadino degli Arienti to Isabella d'Este, Duchess of Mantua.

The composition of the golden ink, determined by means of XRF analysis, is Au/Cu 97–2%, with minor amounts of Hg, K, and Fe, and it is highly consistent throughout the book.

3.3. The Decorative Apparatus

Given the richness and complexity of the decorative apparatus, it is generally accepted that the main artist, namely Marmitta, was assisted by at least three collaborators [23], who were primarily responsible for the decorated initials in folios without miniatures. The characterisation of the palettes, therefore, offers complementary evidence for assessing the materials employed by the different illuminators and for investigating workshop practices. The palettes used by the main artist and by his collaborators were defined by combining the information arising from FORS, XRF, optical microscopy (OM), and HSI. This allowed us to identify a large set of colourants, listed in Table 1.

Table 1. List of colourants identified in the *Offiziolo di Durazzo*.

Colourant	Colour	Technique Used	Artist
Carbon	Black	FORS	All
Azurite	Blue	FORS, XRF, HSI	Marmitta, II and III collaborators
Azurite/ultramarine blue	Blue	FORS, XRF	Marmitta
Ultramarine blue	Blue	FORS, XRF, HSI	Marmitta, I collaborator
Gold	Brown	FORS, XRF	Marmitta
Gold	Gold	FORS, XRF	Marmitta
Azurite/lead-tin yellow type 2	Green	FORS, XRF, HSI	Marmitta
Azurite/verdigris	Green	FORS, XRF, HSI	Marmitta
Iris green	Green	FORS	Marmitta
Lead-tin yellow type 2/copper green	Green	FORS, XRF	Marmitta
Lead-tin yellow type 2/verdigris	Green	FORS, XRF	Marmitta
Malachite	Green	FORS, XRF	Marmitta, III collaborator
Ultramarine blue/lead-tin yellow type 2	Green	FORS, XRF	Marmitta
Unidentified copper green	Green	-	Marmitta
Verdigris	Green	FORS, XRF, HSI	Marmitta
Carbon, silver	Grey	XRF	Marmitta
Realgar	Orange	FORS, XRF	Marmitta
Insect dye	Pink	FORS, HSI	Marmitta
Insect dye	Purple	FORS, HSI	Marmitta
Orchil/vermillion	Red	FORS, XRF	Marmitta
Red ochre	Red	FORS, XRF, HSI	Marmitta
Vermillion	Red	FORS, XRF	All
Insect dye/ultramarine blue	Violet	FORS, XRF	Marmitta
Orchil	Violet	FORS, HSI	Marmitta
Orchil/ultramarine blue	Violet	FORS, XRF	Marmitta
Lead white	White	XRF	All
Lead-tin yellow type 1	Yellow	XRF	Marmitta, II and III collaborators
Lead-tin yellow type 2	Yellow	XRF	Marmitta
Yellow ochre	Yellow	FORS, XRF, HSI	Marmitta

An unusual colourant identified in several instances was realgar (As_4S_4). This pigment was identified in orange areas according to the contextual presence of As and S in the XRF spectrum (Figure 5) and to the inflection point at ca. 525 nm in the FORS spectrum—a feature that cannot be assigned to any other orange pigment. Therefore, even in the absence of fingerprint spectral evidence, such as from Raman analysis, the identification of realgar seems to be reliable.

Lead-tin yellow type 1 and type 2 were characterised by means of XRF analysis, thanks to the contextual presence of, respectively, Pb and Sn or Pb, Sn, and Si. The same evidence resulted from cases where these yellow pigments were used in mixtures with green (verdigris) or blue (azurite, ultramarine blue) pigments.

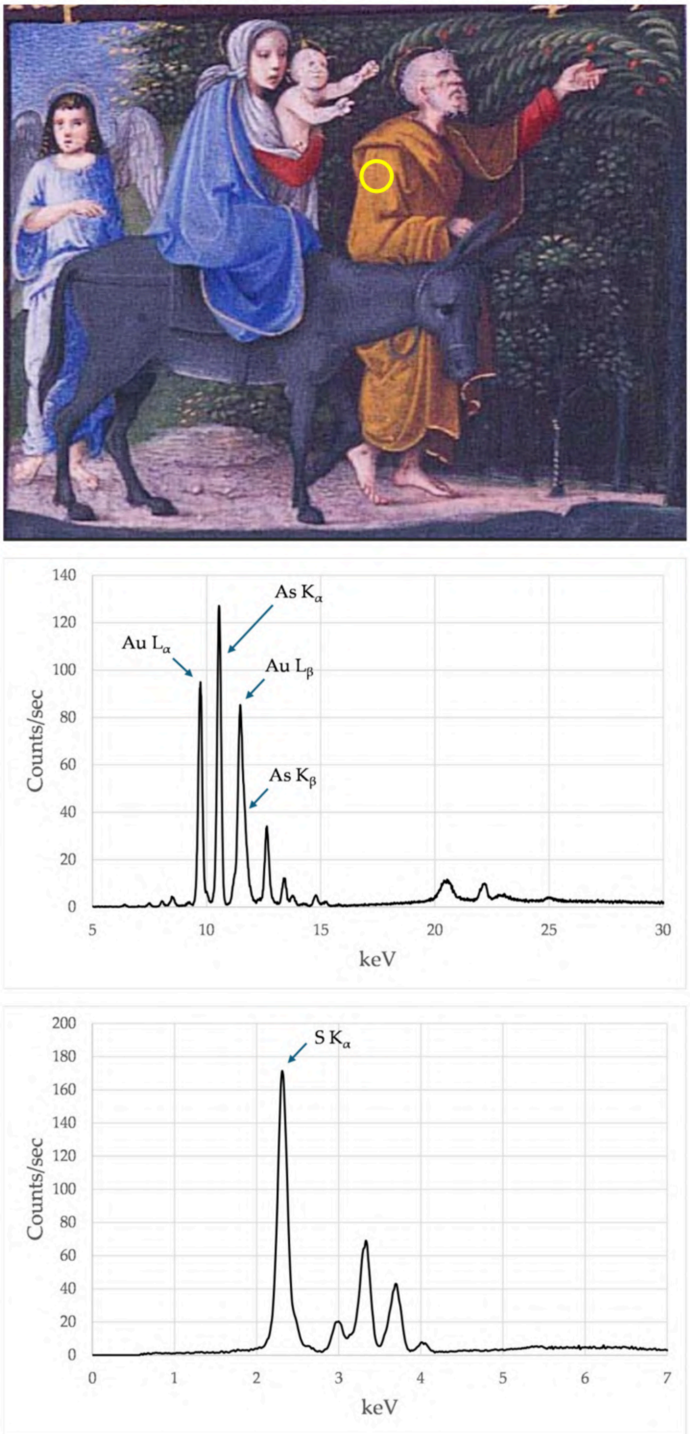

Figure 5. XRF spectrum of the orange coat of St. Joseph ((**top**), f. 76r; the yellow spot indicates the area analysed) in the high-energy range (**middle**) and in the light-energy range (**bottom**).

MBI and HSI Applied to Colour Study

While pigment and dye identification were primarily addressed through FORS and XRF analysis, MBI and HSI data provided complementary information regarding the material spatial distribution, chromatic variability, and manufacturing or conservation-related features.

HSI-derived colorimetric information proved particularly useful to assess the chromatic variability of the purple dye. Although the CIELAB values obtained from hyperspectral data cubes may be affected by limitations associated with the in situ acquisition conditions and by the intrinsic characteristics of parchment substrates, previous validation activities have demonstrated that the adopted methodology provides sufficient accuracy and reproducibility for comparative analyses [24]. Therefore, the present colorimetric results should be primarily interpreted as relative descriptors of chromatic variability within the manuscript, rather than absolute colorimetric measurements.

The mean CIELAB coordinates measured on representative folios are reported in Table 2. The values were derived from 90 representative ROIs (15 × 15 pixels) distributed throughout the manuscript. The resulting values showed relatively consistent chromatic behaviour, supporting the overall coherent distribution of the purple dye.

Table 2. HSI-derived CIELAB colorimetric coordinates (L*, a*, and b*) measured on representative folios of the manuscript. Values reported for each folio correspond to the mean ± standard deviation obtained from three representative regions of interest (ROIs; 15 × 15 pixels each) selected within visually homogeneous purple areas. Summary descriptive statistics (minimum, maximum, mean, median, standard deviation, and interquartile range) are also reported to describe chromatic variability throughout the manuscript.

Folio	L*	a*	b*
2r	28.88 ± 0.84	21.06 ± 0.84	−2.39 ± 0.47
5r	26.87 ± 0.90	16.77 ± 0.53	−8.47 ± 0.53
6r	32.84 ± 1.29	15.65 ± 0.41	−7.94 ± 0.62
8r	27.58 ± 1.12	20.23 ± 1.18	−5.10 ± 0.47
9r	24.68 ± 0.73	20.67 ± 0.42	−2.00 ± 0.43
13r	27.37 ± 0.81	18.16 ± 0.78	−3.08 ± 0.78
13v	19.39 ± 0.88	20.14 ± 0.84	−1.17 ± 0.57
15r	24.26 ± 0.90	23.07 ± 0.99	0.59 ± 0.70
42r	32.63 ± 1.02	17.29 ± 0.64	−0.44 ± 0.47
68r	28.92 ± 0.75	19.81 ± 0.65	−2.04 ± 0.46
72r	33.71 ± 1.20	18.77 ± 0.86	−3.69 ± 1.15
108v	31.38 ± 1.12	21.87 ± 1.15	0.59 ± 0.73
109r	27.67 ± 0.88	23.50 ± 1.34	−2.51 ± 0.79
119r	26.35 ± 0.78	19.32 ± 0.82	0.19 ± 0.39
167r	40.38 ± 1.57	18.26 ± 0.54	0.85 ± 1.10
174v	30.70 ± 0.94	19.79 ± 0.63	0.04 ± 0.57
175r	24.70 ± 0.71	20.12 ± 0.74	−1.64 ± 0.54
193r	17.84 ± 0.57	16.84 ± 0.83	−3.79 ± 0.36
206v	22.24 ± 0.62	24.96 ± 0.75	0.48 ± 0.62
207r	23.54 ± 0.71	22.89 ± 0.81	−0.07 ± 0.43
Min	17.84	15.65	−8.47
Max	33.71	24.96	0.59
Mean	26.93	20.05	−2.23
Median	27.37	20.12	−2.00
SD	4.27	2.43	2.60
IQR	5.34	3.00	3.37

The L* values range from 17.84 to 33.71 (mean = 26.93; median = 27.37; standard deviation, SD = 4.27; interquartile range, IQR = 5.34), while the a* and b* coordinates range, respectively, from 15.65 to 24.96 (mean = 20.05; median = 20.12; SD = 2.43; IQR = 3.00) and from −8.47 to +0.59 (mean = −2.23; median = −2.00; SD = 2.60; IQR = 3.37). The similarity between the mean and median values indicates the absence of strong skewness and confirms the overall chromatic consistency of the manuscript.

As previously observed in validation studies [24,25], the L* coordinate is particularly sensitive to acquisition-related effects associated with the morphology of parchment substrates. Macro- and micro-irregularities of the surface, the local curvature, binding constraints, collagen structural heterogeneity, and consequent non-uniform illumination conditions may affect luminance estimation more strongly than chromatic coordinates, contributing to increased variability among L* values. Therefore, variations observed for L* should be interpreted carefully.

The a* coordinate, associated with the red–green axis, showed limited variability and relatively stable chromatic behaviour along the red component, consistent with the overall visual homogeneity of the purple support. Greater variability was instead observed for b*, where the prevalence of negative b* values indicates that the parchment support generally maintains a bluish chromatic contribution, while the wider distribution along this coordinate suggests that local variations primarily affect the yellow–blue component.

Overall, HSI colorimetry suggests that chromatic variability within the manuscript is relatively limited and largely controlled by subtle local differences rather than by major discontinuities affecting the purple support.

An exception is represented by f. 167v, which exhibits colorimetric coordinates that differ markedly from those of well-preserved folios. In particular, f. 167v is characterised by higher L* values, lower a*, and a shift in b* towards more positive values. These variations indicate a lighter, less saturated, and more yellowish appearance, consistent with the visual observation of faded purple colouration.

In addition to ROI-based colorimetric measurements, HSI-derived a* and b* maps were generated to investigate the spatial distribution of chromatic variations across the parchment surface (Figure 6). The maps provide a spatially resolved representation of the red–green and yellow–blue components (Figure 6b,c, respectively), allowing subtle chromatic heterogeneities to be observed beyond the information obtainable from average colour coordinates alone. These maps are particularly useful for investigating the overall homogeneity of the purple support and for identifying localised chromatic domains associated with differences in dye–substrate interaction, parchment microstructure, or pigment distribution.

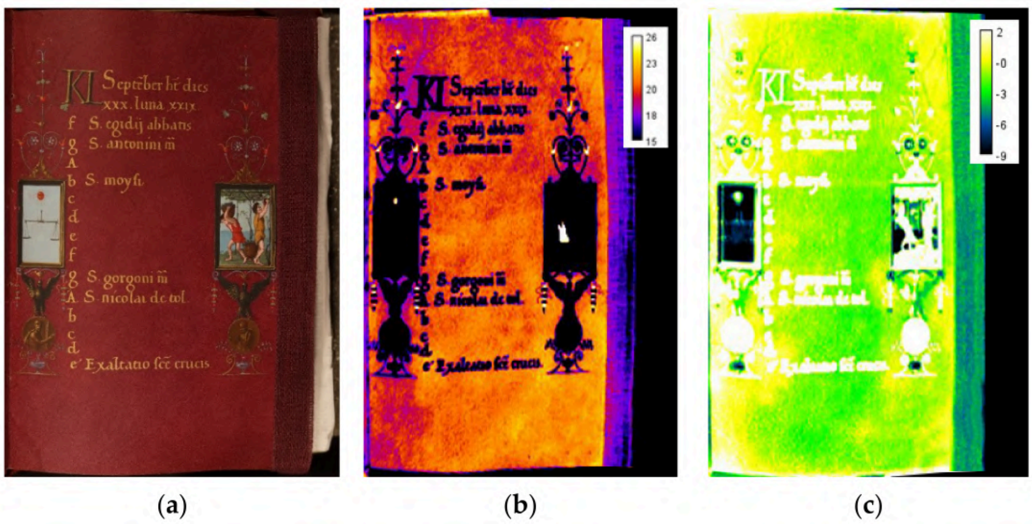

Figure 6. (**a**) VIS image of f. 9r; (**b**) HSI-derived a* map; (**c**) HSI-derived b* map. The colour scales (LUTs) were adjusted to enhance subtle chromatic variations across the parchment surface. Despite minor local fluctuations, both colour coordinates are characterised by limited spatial variability across the parchment surface, supporting the overall uniformity of the purple colouration and indicating the relatively even distribution of the dye.

Most folios showed a remarkably uniform chromatic response, although localised chromatic anomalies and fine-scale spatial patterns in selected areas were observed, which are consistent with subtle variations in the optical behaviour of the purple parchment.

Differential maps of Δa* and Δb* were also generated using a chromatic baseline established from well-preserved areas of the manuscript. By expressing local deviations from this reference condition, the Δa* and Δb* maps suppress much of the natural chromatic variability inherent to the parchment and emphasise changes associated with colour alteration processes (e.g., fading). The differential maps allowed the identification of different behaviours between the well-preserved folios and f. 167v. In the former, the Δa* and Δb* values were generally centred around zero, with mean values of 0.08 and −0.13, respectively, confirming the close agreement between these folios and the reference chromatic condition. At the same time, the relatively large standard deviations (SD = 2.69 for Δa* and SD = 2.84 for Δb*) indicate the presence of localised chromatic variability distributed across the parchment surface.

In contrast, f. 167v was characterised by negative Δa* values (mean = −1.90, SD = 0.48) and positive Δb* values (mean = 3.15, SD = 0.59). The substantially lower standard deviations (SD = 0.48 for Δa* and SD = 0.59 for Δb*) indicate that these chromatic differences are spatially homogeneous and affect most of the folio, rather than being confined to localised areas.

Decorative elements, such as miniatures and ornaments, show considerably greater material complexity, resulting from the use of multiple pigments and mixtures that cannot be adequately described through colorimetric mapping alone.

To support the characterisation of the materials and their spatial distribution, and to assess their homogeneity across the manuscript, the Spectral Angle Mapper (SAM) algorithm, available in the Specim IQ software, was used to classify pixels according to their spectral similarity with selected reference spectra. By comparing spectral signatures on the basis of their shapes, the algorithm generated distribution maps highlighting areas characterised by similar spectral behaviour.

Representative examples are shown in Figure 7, where the IRFC and HSI mapping results enable the spatial visualisation of compositional variability within the miniatures, allowing discrimination between different colourants and colourant mixtures.

(a) (b) (c)

Figure 7. *Cont.*

(**d**) (**e**) (**f**)

Figure 7. (**a**,**d**) VIS images of ff. 174v and 206v; (**b**,**e**) corresponding infrared false-colour (IRFC) images; (**c**,**f**) HSI-derived material maps highlighting the spatial distribution of spectrally distinct blue (**c**) and green paint (**f**) layers.

The combined use of IRFC and hyperspectral mapping suggests the presence of different pigments and/or mixtures within both the miniatures and the surrounding decorative elements. In this framework, UVL also contributed with additional information regarding localised optical responses differing from those of surrounding areas. In Figure 8a,b, localised bright domains affecting selected paint layers can be observed. These features are concentrated along the margins of specific blue regions and exhibit enhanced bluish-white luminescence relative to the surrounding paint. No corresponding variations are evident in the visible images. On the other hand, localised areas characterised by enhanced bluish-white luminescence associated with subtle chromatic variations in visible light are shown in Figure 8c–f.

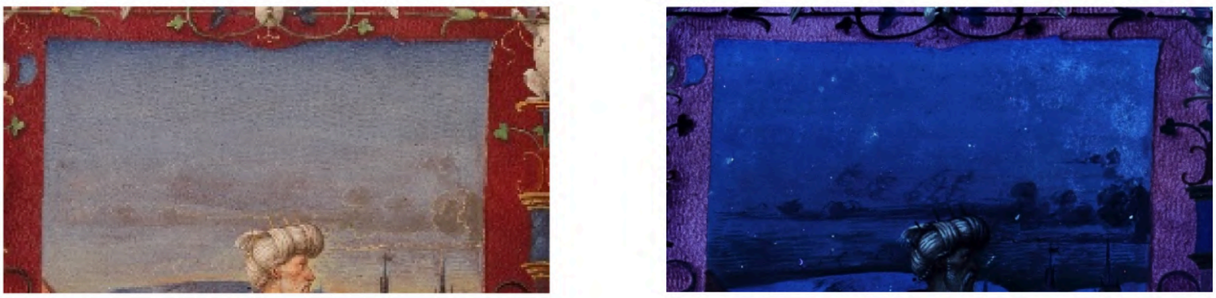

(**a**) (**b**)

(**c**) (**d**)

Figure 8. *Cont.*

(**e**) (**f**)

Figure 8. VIS and UVL images of selected details from the *Offiziolo di Durazzo*. Details from f. 174v (**a**,**b**), f. 118v (**c**,**d**), and f. 15r (**e**,**f**). The UVL images reveal differences in luminescence behaviour associated with the paint layer and/or conservation works.

3.4. The Gold and Silver Binding

The precious binding of the *Offiziolo di Durazzo*, coeval of the manuscript, is the key feature that allowed scholars to identify it inside the *Portrait of a Collector* painting by Parmigianino. It was created in chiselled silver with golden parts. The composition of the silver alloy is Ag/Cu 87.7–11.2%, with traces (<1%) of Cr, Fe, Pb, Sn, and Zn. The golden parts were decorated by means of the fire gilding technique, i.e., using a gold/mercury amalgam, as is apparent from the Hg L_α and L_β lines in the XRF spectrum (Figure 9).

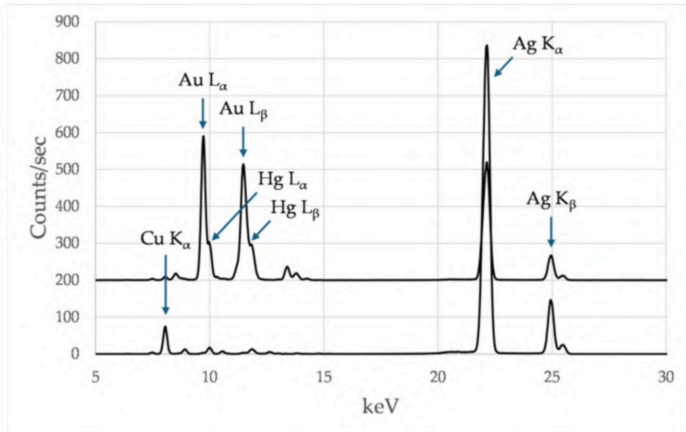

Figure 9. XRF spectra from a silver part (bottom line) and a golden part (top line).

The two staples on the front edge of the front plate are decorated with two red gemstones that, curiously, have always been described as rubies [23,26], while the FORS analysis revealed that they were apparently pyrope–almandine garnets according to the typical absorption maxima at 413, 431, 500, 541, 575, 611 (shoulder), and 690 nm [27]. It is suggested, however, that they could have been replacement parts for the original gemstones.

4. Discussion

4.1. The Purple Parchment

The use of the purple colour sought to recall the tradition and symbolism of Late Antique and early medieval purple codices—examples of book production intended for the highest social classes of these times. Marmitta had previously used this feature in the making of the *Messale della Rovere* or *Messale Marmitta* (ms. 466/M, Turin, Museo Civico di Arte Antica), a missal produced together with other two artists between 1490 and 1492 on commission by the Italian Cardinal Domenico della Rovere. This richly decorated missal contained three purple leaves (ff. 7bis, 140bis, and 247bis); in keeping with the Late Antique and early medieval traditions, the dye used for the purple was orchil. The same dye was used in the *Offiziolo di Durazzo.* One wonders, however, how Marmitta knew that this was precisely the dye used almost 1000 years earlier by the Byzantine artisans who produced the purple codices; it should be noted that, in other volumes contemporary with the *Offiziolo di Durazzo* and also containing purple pages, the dyes used were different, likely a function of the raw materials available locally. The explanation, perhaps, is linked to the artist's knowledge of the very few sources that report the procedure for dyeing parchment with orchil, most likely including the *Praecepta colorum* by Felice Feliciano (1460, cod. Vat. lat. 6852, Vatican City, Vatican Apostolic Library). Alternatively, he may have been in contact with artists who had already used orchil for this purpose, such as Bartolomeo Sanvito for the *Uffiziolo di Bianca Maria Visconti* (1475, ms. S.P. 13, Milan, Biblioteca Ambrosiana) and the *Book of Hours of Cardinal Carafa* (1480, ms. Vat. lat. 9490, Vatican City, Vatican Apostolic Library).

The identification of orchil is particularly relevant from a conservation point of view. In fact, this dye, as with most natural dyes, is fugitive, i.e., it tends to fade when exposed to improper light conditions [28]. Therefore, information concerning its identification is important when determining the conditions for illumination in the event of displaying the manuscript to the public.

Orchil Distribution and Parchment–Dye Interaction

Following the identification of orchil as the primary purple colourant through FORS analysis, a combined imaging approach further allowed the evaluation of chromatic variability and local heterogeneity, providing insights into differences in dye distribution, application uniformity, and conservation-related alterations. HSI-derived colorimetric maps (L*, a*, b*) also allowed an investigation of colour variability across the manuscript [29].

Overall, the purple colouration showed substantial homogeneity, supporting a relatively coherent dyeing process, as observed in Figure 10, where the HSI-derived colorimetric coordinates a* and b* are reported.

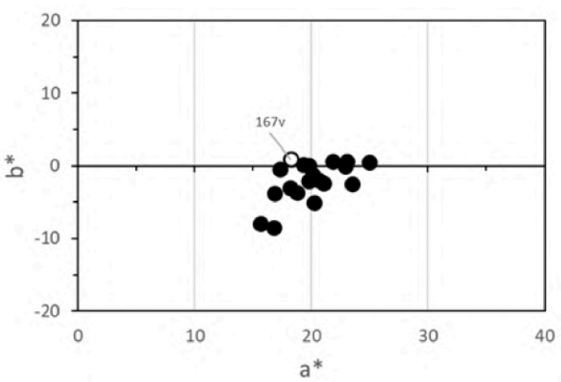

Figure 10. Scatter plot of the average a* and b* colour coordinates measured on selected folios. The white marker corresponds to folio f. 167v, whereas black markers represent well-preserved pages.

HSI-derived colorimetric maps of the a* and b* coordinates provide a useful tool for investigating the spatial distribution and optical behaviour of purple dyes on parchment substrates. Unlike point-based colour measurements, spatially resolved colorimetric imaging enables the visualisation of local chromatic heterogeneity, revealing micro-variations that may reflect differences in dye penetration, retention, interaction with the collagen matrix, and alteration.

In purple-dyed parchments, colour appearance is not controlled exclusively by the intrinsic spectral properties of the dye but also by the complex optical interaction between the dye and the parchment substrate [28]. Since the dye is partially absorbed within the collagen fibre network, rather than forming a perfectly homogeneous superficial layer, local variations in collagen microstructure, fibre orientation, porosity, and surface compaction can significantly influence the resulting reflectance behaviour.

Within this framework, a spatially resolved colour investigation is particularly significative. While the a* coordinate reflects the red–magenta contribution of the purple dye layer, b* is more sensitive to variations in the balance between the bluish-violet chromatic component of the dye and the yellowish contribution of the underlying parchment substrate [30,31]. The combined spatial analysis of these coordinates can therefore provide valuable insights into localised chromatic heterogeneities associated with variations in dye distribution, dye–substrate interaction, and support-related optical effects. HSI-derived a* and b* maps reveal subtle spatial patterns that are often imperceptible under visible observation alone, allowing technologically or structurally induced heterogeneities to be visualised and correlated with features observed through complementary imaging techniques such as UVL.

Overall, the manuscript is characterised by a homogenous chromatic appearance. The HSI-derived a* and b* maps obtained from f. 9r (Figure 6) provide a representative example of this behaviour. Both maps display relatively uniform colour distributions across most of the parchment surface, with only limited localised fluctuations. The high average a* value (20.67) indicates a generally strong red contribution of the purple dye layer, while the negative b* values are consistent with the bluish-violet (magenta) component characteristic of well-preserved orchil-dyed parchment. The relatively low variance observed for both a* (0.62) and b* (0.38) further confirms the limited chromatic variability of the folio. Although subtle spatial heterogeneities remain visible in the colour maps, no large-scale chromatic domains or abrupt transitions can be observed, supporting the overall homogeneity of the purple support.

The remarkable chromatic homogeneity observed throughout the manuscript may reflect the combination of a controlled dyeing process and a relatively uniform interaction between the orchil dye and the parchment substrate [28]. The absence of systematic differences between flesh and grain sides further suggests that substrate-related optical effects do not dominate the overall chromatic response at the manuscript scale.

To further investigate localised colour alterations, differential maps of Δa^* and Δb^* were generated by subtracting the average a* and b* values measured in well-preserved areas of the manuscript from each pixel of the HSI-derived colour maps [32]. These maps highlight local deviations from the reference chromatic state, allowing the visualisation of colour changes affecting the purple dye. The contrast between the well-preserved f. 9r and the faded f. 167v is particularly evident. As shown in Figure 11a–c, f. 9r shows Δa^* and Δb^* values that are generally close to zero, indicating a chromatic response consistent with the reference condition and only limited spatial variability.

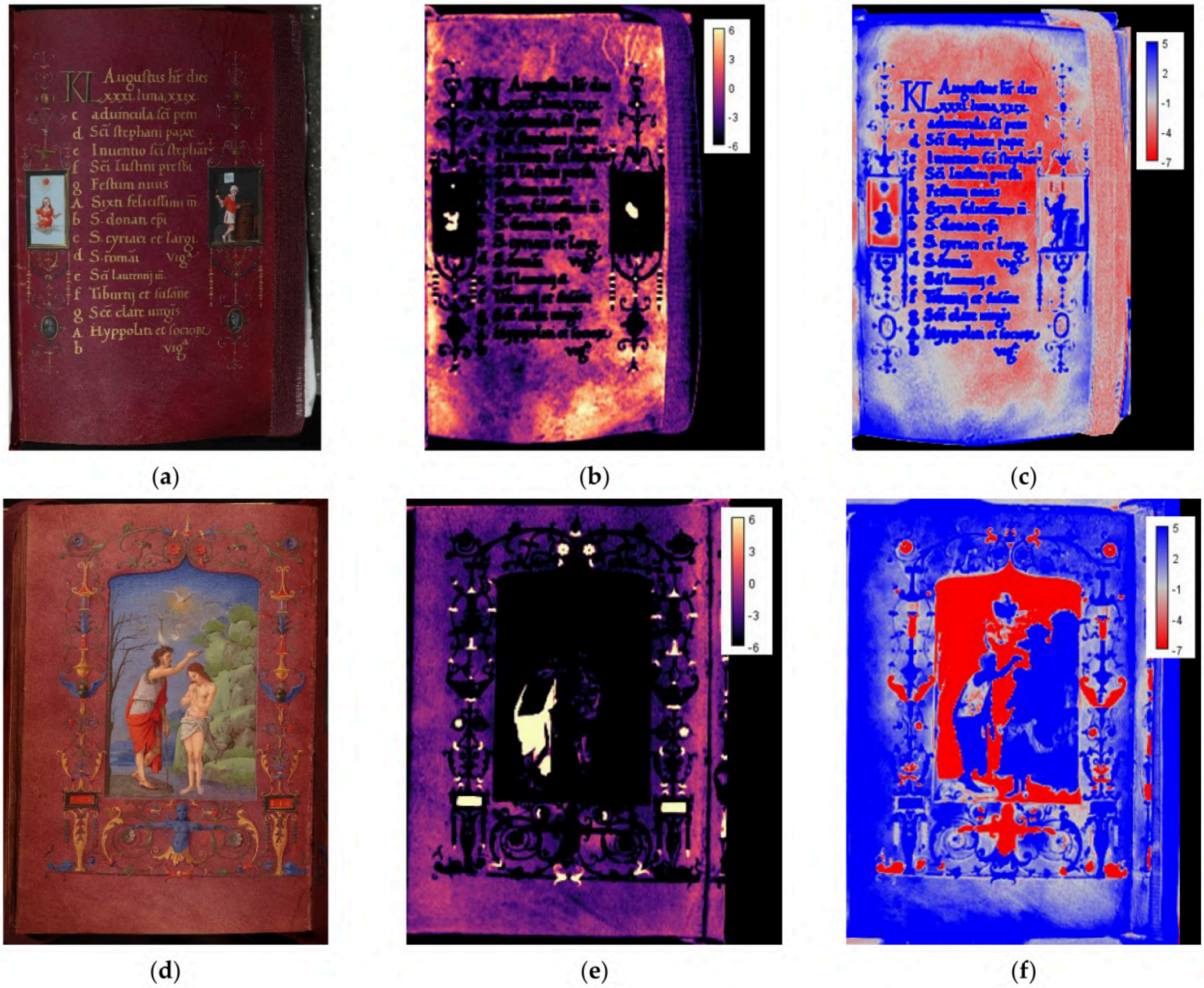

Figure 11. Comparison between a well-preserved folio (9r, **a**–**c**) and f. 167v (**d**–**f**) affected by colour fading. (**a**,**d**) VIS images; (**b**,**e**) Δa* maps; (**c**,**f**) Δb* maps. The colorimetric maps were generated from HSI data and visualised using fixed LUT scales to allow direct comparison between folios.

While f. 9r (Figure 11a–c) shows only minor deviations from the reference condition, f. 167v (Figure 11d–f) is characterised by extensive positive Δb* values and strongly negative Δa* values. The altered areas form broad and coherent domains, revealing a large-scale chromatic modification affecting most of the exposed surface. Relative to the reference condition, this behaviour is characterised by a marked decrease in the red component, accompanied by an increase in the yellow contribution. These changes are consistent with photo-induced fading and are compatible with the documented prolonged exposure of this folio to natural light.

MBI and HSI imaging also revealed subtle localised heterogeneities within the purple parchment that that are not readily explained by the extensive degradation of the colourant [17,28]. The spatial distribution of these features, together with their behaviour in the UVL images and HSI-derived a* and b* maps, is more consistent with local variations in the parchment support and its interaction with the purple dye than with localised fading phenomena [33].

The heterogeneous distribution of spot-like domains is clearly visible throughout the parchment in f. 13r (Figure 12a–d). The colorimetric maps show higher a* values in these areas, suggesting a a stronger red–violet chromatic contribution exerted by the purple dye, together with a reduced influence of the parchment substrate. Their rounded morphology, spatial organisation, and limited correspondence with luminance variations suggest localised differences in dye absorption, retention, or superficial distribution rather than large-scale chromatic alterations.

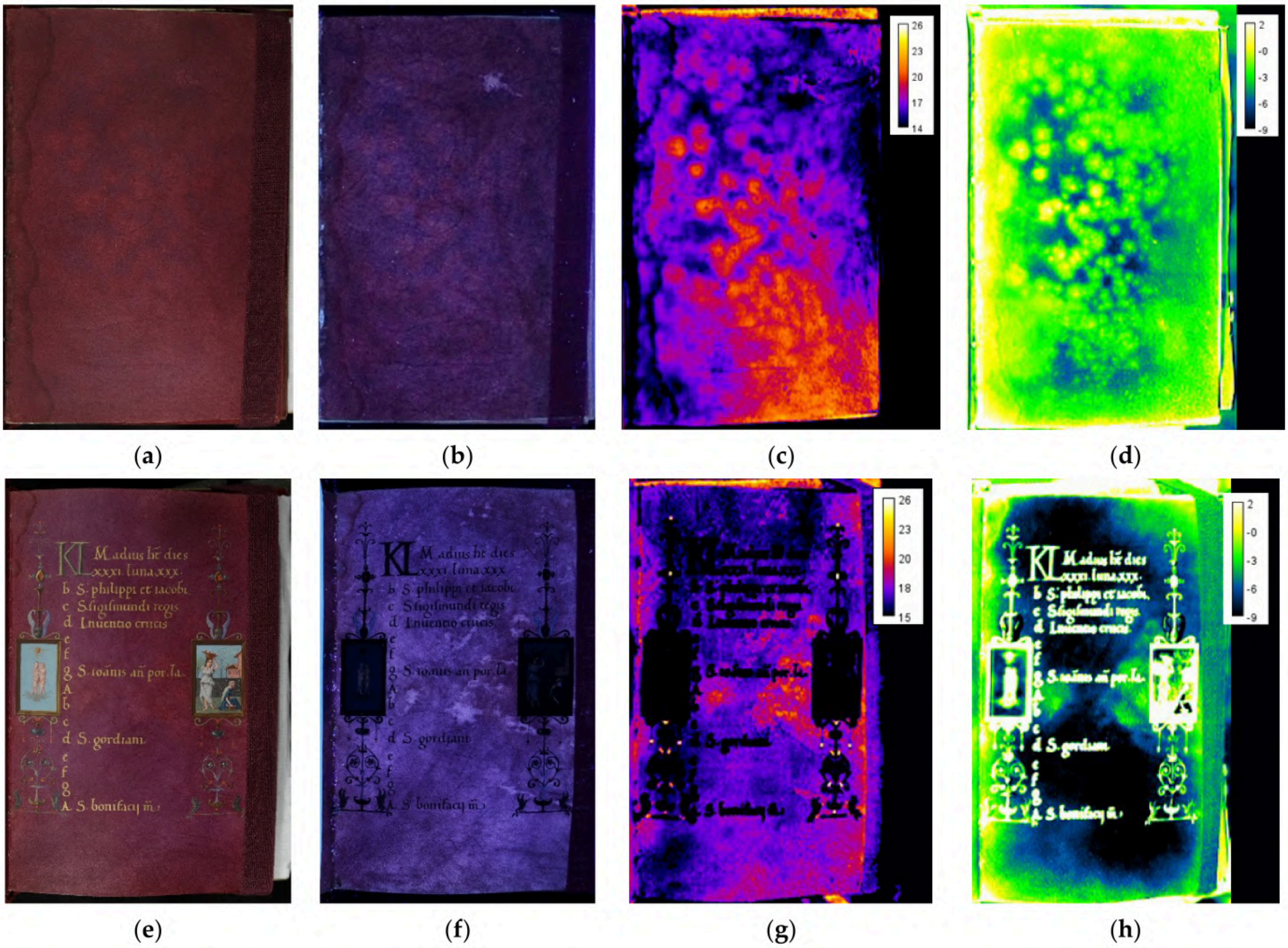

Figure 12. Comparison of VIS, UVL, and HSI-derived a* and b* maps of ff. 13r (**a**–**d**) and 5r (**e**–**h**). The colorimetric maps were generated from HSI data and visualised using fixed LUT scales to allow direct comparison between folios.

Such behaviour may reflect the influence of natural microstructural heterogeneities within the parchment, including local variations in collagen fibre density, porosity, surface morphology, residual follicular microrelief, and compaction induced during manufacture [33]. These factors can influence the interaction between the dye and the collagen matrix, producing localised variations in colour and optical response that become particularly evident in UVL imaging. Indeed, while the associated colour differences remain relatively subtle in the HSI-derived maps, UVL enhances these features owing to the combined contribution of the dye distribution, substrate properties, UV absorption, and luminescence behaviour.

In contrast, the UVL image of f. 5r reveals marked spatial heterogeneity across the purple parchment (Figure 12e,f), characterised by irregular brighter and darker domains distributed throughout the support. A comparison with the corresponding HSI-derived a* and b* maps indicates that areas exhibiting enhanced luminescence generally correspond to locally higher a* values, whereas weaker correspondence is observed for b*. This behaviour suggests that the UVL pattern cannot be explained solely by chromatic differences or localised dye loss.

The spatial organisation of these features, together with their colorimetric behaviour, may suggest a strong influence of substrate-related factors on the optical response of the dyed parchment [28]. Similar heterogeneities have been observed in other folios and are consistent with localised variations in the interaction between the orchil dye and the parchment substrate. Natural microstructural heterogeneities inherited from the original dermal anatomy and further modified during parchment manufacture may influence dye uptake, retention, and optical behaviour, producing regions characterised by a stronger chromatic contribution of the dye layer without substantial changes in luminance.

At the same time, local differences in parchment structure may affect UV absorption, internal scattering, and dye–substrate optical interactions, thereby enhancing luminescence contrast. Consequently, the patchy UVL response likely reflects the combined effect of the dye distribution and parchment microstructure, rather than simple substrate exposure or the extensive degradation of the colourant. These observations highlight the sensitivity of UVL imaging to subtle variations in the optical relationship between the orchil dye and the collagen-based support, providing information that complements the colorimetric patterns revealed by HSI mapping.

The combined analysis of UVL images and HSI-derived colorimetric values also provides valuable clues for interpreting the anomalous optical behaviour observed in Figure 4c. In folios where the writing area is surrounded by a decorative frame (e.g., ff. 15r, 72r, 109r, 119r, 175r, and 207r), subtle but systematic chromatic differences were detected between the central panel and the outer border, with the latter appearing generally darker and more chromatically saturated. These differences correspond to average values of $\Delta L^* = 1.64$, $\Delta a^* = -0.46$, $\Delta b^* = -1.70$ ($\Delta E00 = 2.14$). These variations may reflect differences in dye absorption related to parchment preparation, localised retouching or reinforcement of the purple background, or variations in the interaction between the dye and the collagen substrate.

4.2. The Golden Text

The extraordinary skill of the calligrapher Pietro Antonio Sallando is attested to by the absence of errors or second thoughts in the writing—both characteristics that would have caused the precious purple parchment to be wasted. However, while other books are known in which Sallando was at work, such as a purple *Offiziolo* kept at the Bodleian Library in Oxford (ms. Canon. Liturg. 287), in which Sallando collaborated with Marmitta, or the *Libro d'ore Ghislieri* (ms. Yates Thompson 29, London, British Library), written for the Bolognese nobleman Bonaparte Ghislieri around 1500, unfortunately, no diagnostic studies have been carried out on these artworks, so it is not possible to perform a comparison regarding the composition of his inks.

4.3. The Decorative Apparatus

The first consideration regarding the decorative apparatus is that the palette of Marmitta was very rich in terms of precious colourants: gold, silver, ultramarine blue, vermilion, insect dyes, and malachite all ranked highly on the price lists of colourant dealers in the Renaissance, as far as is known from bibliographic sources [34–38]. Particularly meaningful was the use of the expensive ultramarine blue pigment, obtained from the semi-precious lapis lazuli rock: according to a theory of Delamare [39], supported by Kirby [40], the trade of the lapis lazuli rock from the mines of Badakshan (present-day Afghanistan) to Europe could have been blocked by the fall of Constantinople in 1453. Therefore, the presence of ultramarine blue in the *Offiziolo di Durazzo* must be seen as an indication of the extraordinary availability of resources.

It is interesting to compare the palette of the *Offiziolo di Durazzo* with that used by Marmitta in the already cited *Messale della Rovere* (1490–1492, ms. 466/M, Turin, Museo Civico di Arte Antica), the only book attributed to Marmitta that has been subjected to a diagnostic study and therefore the only one available for comparison. In Table 3, the palettes of the two manuscripts are shown; for the *Messale della Rovere*, only the data relative to the section decorated by Marmitta are reported (it is known that other two artists contributed [41]).

Table 3. Palettes in the *Offiziolo di Durazzo* and in the *Messale della Rovere*.

Colour	*Offiziolo di Durazzo*	*Messale della Rovere*
Black	Carbon	Carbon, IGI
Blue	Ultramarine blue, azurite, azurite/ultramarine blue	Ultramarine blue, azurite, azurite/ultramarine blue
Brown	Gold	Vermillion, vermillion/lead-tin yellow type 2, gold, red ochre, yellow ochre
Gold	Gold	Gold
Green	Azurite/lead-tin yellow, azurite/verdigris, iris green, lead-tin yellow/copper green [1], lead-tin yellow/ultramarine blue, lead-tin yellow/verdigris, malachite, verdigris	Malachite, verdigris, lead-tin yellow/ultramarine blue
Grey	Carbon, silver	Carbon
Orange	Realgar	Yellow ochre
Pink	Insect dye	Insect dye
Purple	Insect dye	Vermillion/insect dye, insect dye, folium
Red	Vermillion, red ochre	Vermillion, red ochre
Violet	Insect dye/ultramarine blue, orchil, orchil/ultramarine blue	Folium, folium/ultramarine blue
White	Lead white	Lead white
Yellow	Lead-tin yellow type 1, lead-tin yellow type 2, yellow ochre	Lead-tin yellow type 2, vermillion/malachite/lead-tin yellow type 2

[1] Unidentified colourant.

Assuming that the two artworks are attributed to the same artist on a stylistic basis, the palette of the *Offiziolo of Durazzo* is somewhat more varied and evolved, possibly as a consequence of the technical evolution of the artist and/or of the wider availability of materials, such as iris juice, realgar, and silver. Generally speaking, the use of different mixtures of colourant is remarkable and indicative of a very advanced and refined painting technique.

Among the various colourants, the use of realgar is noteworthy: this pigment, in fact, was rarely used in the Middle Ages and the Renaissance and was mostly used in Middle Eastern Asian paintings. Lucas Cranach the Elder, a contemporary of Marmitta, made frequent use of it, having it available in his pharmacy in Wittenberg [42]. Among the few identifications reported, we can mention the mid-6th-century Syriac manuscript known as *Rabbula Gospels* (ms. Plut. I 56, Florence, Biblioteca Medicea Laurenziana) [43]; ms. Add. MS 7170, an illustrated 13th-century West Syriac lectionary (London, British Library) [44]; and a few late Islamic manuscripts cited by Knipe et al. [45]. In all cited cases, it was possible to confirm the availability of local resources of the mineral. In the case of the *Offiziolo di Durazzo*, one can cite the Cetine di Cotorniano mine in Tuscany, not far from Parma.

As for the collaborators of Marmitta, the results of the analyses allow us to characterise them as follows:

- The first one is active in the decorated initials at ff. 64r-73v and uses carbon, vermillion, and ultramarine blue;
- The first one is active in the decorated initials at ff. 64r-73v; he uses carbon, vermillion, and ultramarine blue;
- The second one is active in the decorated initials at ff. 74r-123v, 154r-193v, and 204r-213v and in some initials, together with collaborator III, at ff. 194r-203v; he uses azurite, carbon, lead-tin yellow, and vermillion;
- The third one is active in the decorated initials at ff. 124r-153v and in some initials, together with collaborator II, at ff. 194r-203v; he uses azurite, carbon, lead-tin yellow, malachite, and vermillion.

While the FORS analysis provided the basis for pigment identification, the integration of HSI and MBI data was used for a more comprehensive assessment of the spatial distribution of pigments and paint mixtures within the miniatures. The SAM classification maps revealed the presence of multiple spectrally distinct domains that only partially correspond to the colour differences visible to the naked eye, highlighting the complexity of the painting technique. In several cases, areas characterised by a similar visual appearance were found to be composed of different pigment mixtures.

Among the analysed colours, green and blue areas showed the greatest spectral variability in the FORS dataset and were therefore selected for a more detailed investigation through imaging techniques. Representative examples are provided by ff. 174v and 206v (Figure 6), where the SAM classification maps reveal the coexistence of several spectrally distinct domains corresponding to different pigments and paint mixtures.

The results are summarised in Table 4, which reports the main spectral classes identified through HSI mapping, together with their proposed interpretations based on the combined evaluation of the FORS, VIS, UVL, IR, and IRFC data. Rather than representing individual pigments alone, several classes correspond to mixtures used to modulate hue, saturation, and brightness. In particular, the blue and green paint layers show a heterogenous combination of ultramarine, azurite, white pigments, and copper-based greens, reflecting the deliberate exploitation of different optical properties to achieve specific chromatic effects.

Particularly interesting are the SAM classes displayed in yellow. Their reflectance spectra exhibit the characteristic orchil absorption bands at approximately 545 and 595 nm, while the higher overall reflectance suggests the additional contribution of lead white and possibly minor amounts of azurite. The imaging data indicate that these areas cannot be interpreted as a simple pigment mixture. Their transparency in the infrared image argues against significant concentrations of azurite, whereas the light pink appearance in IRFC is compatible with mixtures dominated by ultramarine and white pigments. At the same time, the UVL response more closely resembles that of areas containing both ultramarine and azurite. Taken together, these observations suggest a complex paint formulation involving orchil, likely responsible for the pale violet appearance, in combination with white pigments and possibly small amounts of blue pigments.

Overall, the mapping results demonstrate that a varied palette of blue and green mixtures was used throughout the decorative apparatus.

A peculiar feature was observed in the blue sky at f. 174v (Figure 7a,b), where UVL imaging reveals a series of localised brighter domains distributed across the paint layer, particularly in the upper-right portion of the scene. These features exhibit a diffuse, irregular morphology and are clearly visible under UV excitation, whereas they are barely perceptible in the VIS image. Moreover, no corresponding variations can be identified in the IRFC image or in the HSI-derived a* and b* maps. The absence of significant colorimetric or spectral differences suggests that these domains are unlikely to be associated with major variations in pigment composition.

Table 4. Summary of the spectral classes identified through SAM classification of HSI data in the miniatures of ff. 174v and 206v. For each class, the proposed material attribution is reported together with the supporting evidence derived from the combined interpretation of FORS, VIS, UVL, IR, and IRFC data.

SAM Class	Visual Appearance	MBI	Composition
Light blue	Blue and light blue	Transparent in IR; light pink in IRFC; weak-to-moderate UVL response	Ultramarine ± lead white
Blue	Dark blue areas	Partial IR attenuation; reddish-pink IRFC response; relatively low UVL emission	Azurite + ultramarine
Green	Light blue	Transparent in IR; pink IRFC response similar to ultramarine-rich areas; homogeneous UVL response	Ultramarine + white pigment
Pink	White	High reflectance in VIS and IR; bright in IRFC; weak UVL response	Lead white
Yellow	Pale violet	Transparent in IR; light pink in IRFC; enhanced UVL response comparable to ultramarine–azurite mixtures	Orchil + white pigment ± minor azurite
Purple	Green	Intermediate IR attenuation; distinct IRFC behaviour relative to blue mixtures; limited UVL emission	Azurite + yellow pigment
White	Light green	Variable IR behaviour; spectrally distinct from ultramarine-based mixtures; UVL response not diagnostic	Copper-based green + yellow pigment
Orange/red	Green	Moderate IR absorption; characteristic response of copper-containing paint layers; weak UVL emission	Copper-based green

Instead, the observed pattern may reflect localised enrichment phenomena involving the organic binding medium [46]. The redistribution or accumulation of binder components at the paint surface can significantly affect UV-induced luminescence while producing only minor or undetectable changes in visible reflectance properties. The diffuse morphology of these features, their preferential occurrence within specific portions of the blue paint layer, and their enhanced UVL response are therefore more consistent with modifications affecting the organic fraction of the paint rather than the pigment itself.

A possible explanation involves migration processes occurring within tempera paint systems. An imbalanced pigment-to-binder ratio, incomplete mixing, or long-term physicochemical evolution of the paint film may promote the movement of mobile organic components toward the surface, generating bloom- or efflorescence-like features [47]. Such processes may occur independently of light exposure and can be favoured by restricted air circulation and stable environmental conditions [46]. Under these circumstances, localised surface enrichment of proteinaceous or polysaccharide-rich materials may develop, producing areas of enhanced UV-induced luminescence without substantially altering the visible appearance or spectral response of the underlying pigment layer.

4.4. Limitations of Hyperspectral Imaging

Although HSI proved to be a powerful tool for investigating the spatial distribution of the materials and conservation-related features throughout the manuscript, some methodological limitations should be considered when interpreting the results.

Hyperspectral imaging allows the recording of the reflectance spectrum at each image pixel, enabling the recognition of areas characterised by similar spectral behaviour. The main limitation of reflectance hyperspectral imaging for material identification does not primarily arise from the spectral resolution, which is generally sufficient to resolve the absorption features of most historical pigments in the visible–near-infrared range. Rather, it results from the intrinsic complexity of historical paint layers, where each pixel records the combined spectral response of pigments, binders, degradation products, and the underlying substrate [5,10,19,48]. Additional uncertainty arises from the spectral overlap among different materials and from the limited spectral range (400–1000 nm), which excludes diagnostic absorption features located in the short-wave infrared region. Consequently, HSI is more appropriately regarded as a technique for mapping spectral similarity than for providing unambiguous material identification. In the present study, the identification of pigments and dyes was thus primarily supported by FORS, which provided diagnostic molecular information, and by XRF, which supplied complementary elemental data.

A further limitation concerns the spectral similarity of different materials. Organic colourants, mixtures of pigments, and degraded compounds may exhibit partially overlapping absorption/reflectance features, reducing the discriminating capabilities of hyperspectral data alone. This aspect is particularly relevant for historical manuscripts, where alterations induced by ageing, previous conservation treatments, or binder modifications may further modify the original spectral response.

The quality of hyperspectral data is also influenced by the acquisition conditions. The illumination geometry, working distance, surface curvature, local gloss, and variations in parchment topography may affect the recorded reflectance spectra [24,25,49]. Although the acquisition protocol adopted in this study was specifically designed to minimise these effects, small variations in illumination and surface orientation cannot be completely eliminated during in situ measurements on bound manuscripts.

For these reasons, the classification maps presented in this work should be interpreted as representations of spectral similarity rather than absolute material maps. The SAM algorithm identifies pixels whose spectra are compatible with selected reference signatures, but the reliability of the resulting classification depends on the quality of the reference spectra, the selected similarity threshold, and the spectral separability of the investigated materials. Accordingly, the HSI results were interpreted only where they were consistent with the independent evidence provided by the FORS and XRF analyses.

Despite these limitations, HSI remains an extremely valuable tool for the study of illuminated manuscripts. Its potential mainly lies in the ability to extend the information obtained from point-based spectroscopic techniques to the entire manuscript surface, enabling the spatially resolved visualisation of material distributions, technological features, and conservation-related phenomena. Within an integrated multi-analytical workflow, HSI therefore represents a powerful complement to spectroscopic techniques, rather than a replacement for them.

5. Conclusions

A combined, entirely non-invasive approach involving the FORS, XRF, MBI, and HIS techniques allowed us to increase the knowledge of the manufacturing of the *Offiziolo di Durazzo* and to obtain information that is useful to determine the appropriate conditions for storage and exposition. The results of the analyses clarify the extremely varied, rich, and complex palette used by Francesco Marmitta, together with the simpler palettes used by his three collaborators. Inside the decorative apparatus, the combined interpretation of MBI and HSI spectral mapping allowed the visualisation of the colourant distribution and paint mixtures, providing insights into artistic techniques, material selection, and workshop practices.

The precise identification of orchil as the dye used to impart the purple colour to the parchment will enable those in charge of the conservation of the manuscript to better manage the conditions under which it is stored and displayed. In fact, orchil, in contrast to the more lightfast Tyrian purple dye, is fugitive, i.e., it tends to fade due to interactions with external light. In actuality, the manuscript is stored in complete darkness, but, in the event of requests for display, this information will be relevant in assessing them.

Author Contributions: Conceptualisation, M.A. and M.P.; methodology, C.F.; software, E.C.; validation, A.A. and E.C.; formal analysis, M.A., M.P., C.F. and A.A.; investigation, E.C.; resources, E.F.; data curation, C.F.; writing—original draft preparation, M.A., E.F. and C.F.; writing—review and editing, M.P. and A.A.; visualisation, E.C.; supervision, E.F.; project administration, M.P.; funding acquisition, M.A. All authors have read and agreed to the published version of the manuscript.

Funding: This research was funded by the project PURPLE—Purple Parchment Legacy: Art History and Heritage Science for the Study of Manuscript Painting from Late Antiquity to the Modern Age (5th–19th centuries)—financed by PRIN: Progetti di Ricerca di Rilevante Interesse Nazionale—competition 2020, Protocol n. 2020P8W99T, Sector ERC SH5, CUP C93C22000530001.

Institutional Review Board Statement: Not applicable.

Informed Consent Statement: Not applicable.

Data Availability Statement: Dataset available on request from the authors.

Acknowledgments: The authors would like to acknowledge Simonetta Castronovo, curator of the manuscript collection at Museo Civico di Arte Antica in Turin, for allowing a thorough inspection of the *Messale della Rovere*. Elena De Laurentiis is kindly acknowledged for all suggestions and fruitful discussions.

Conflicts of Interest: The authors declare no conflicts of interest. The funders had no role in the design of the study; in the collection, analyses, or interpretation of the data; in the writing of the manuscript; or in the decision to publish the results.

References

1. De Marchi, A. *Il Libro D'ore Durazzo: Volume Di Commento*; Franco Cosimo Panini: Modena, Italy, 2008; ISBN 978-88-248-0444-8.
2. Malfatto, L. Una Biblioteca in Tempo Di Guerra: La Berio Dal 1935 al 1947. *Atti Della Soc. Ligure Di Stor. Patria* **2025**, *LXV*, 107–187.
3. Cappa, F.; Paganoni, I.; Carsote, C.; Schreiner, M.; Badea, E. Studies on the Effect of Dry-Heat Ageing on Parchment Deterioration by Vibrational Spectroscopy and Micro Hot Table Method. *Polym. Degrad. Stab.* **2020**, *182*, 109375. [CrossRef]
4. Chlebda, D.K.; Rogulska, A.; Łojewski, T. Assessment of Hyperspectral Imaging System for Colour Measurement. *Spectrochim. Acta-Part A Mol. Biomol. Spectrosc.* **2017**, *185*, 55–62. [CrossRef] [PubMed]
5. Cucci, C.; Delaney, J.K.; Picollo, M. Reflectance Hyperspectral Imaging for Investigation of Works of Art: Old Master Paintings and Illuminated Manuscripts. *Acc. Chem. Res.* **2016**, *49*, 2070–2079. [CrossRef] [PubMed]
6. Chakravarty, S.; Paikaray, B.K.; Mishra, R.; Dash, S. Hyperspectral Image Classification Using Spectral Angle Mapper. In Proceedings of the 2021 IEEE International Women in Engineering (WIE) Conference on Electrical and Computer Engineering (WIECON-ECE), Dhaka, Bangladesh, 4 December 2021; pp. 87–90.
7. *CIE 15:2004 Technical Report. Colorimetry*, 3rd ed.; Commission International de I'Eclairage (CIE): Vienna, Austria, 2004.
8. *ISO/CIE 10526 CIE Standard*; Colorimetric Illuminants. International Organization for Standardization: Geneva, Switzerland, 1991.
9. *ISO/CIE 10527 CIE Standard*; Colorimetric Observer. International Organization for Standardization: Geneva, Switzerland, 1991.
10. Cherubini, F.; Casini, A.; Cucci, C.; Picollo, M.; Stefani, L. Application of a Hyperspectral Camera for Colorimetric Measurements on Polychrome Surfaces in a Controlled Environment and Evaluation of Three Image Processing Software for Displaying Colorimetric Data: Pros and Cons of the Methodology Presented. *Color Res. Appl.* **2022**, *48*, 210–221. [CrossRef]
11. Webb, E.K.; Herrero-Cortell, M.À.; Picollo, M. (Eds.) *Multiband Imaging Techniques with Silicon-Based Sensors*; EdUPV Editorial Universitat Politècnica de València: Valencia, Spain, 2025; ISBN 978-84-1396-223-8.
12. Cortea, I.M.; Ghervase, L.; Ratoiu, L.; Rădvan, R. Application of Spectroscopic and Hyperspectral Imaging Techniques for Rapid and Nondestructive Investigation of Jewish Ritual Parchment. *Front. Mater.* **2020**, *7*, 601339. [CrossRef]

13. Salvadori, C. *Non-Invasive Techniques Applied to Cultural Heritage: Raman Spectroscopy and X-Ray Fluorescence for the Study of Medieval Manuscripts*; Università Ca' Foscari Venezia Open Archive: Venice, Italy, 2016.
14. Aceto, M.; Agostino, A.; Fenoglio, G.; Idone, A.; Gulmini, M.; Picollo, M.; Ricciardi, P.; Delaney, J.K. Characterisation of Colourants on Illuminated Manuscripts by Portable Fibre Optic UV-Visible-NIR Reflectance Spectrophotometry. *Anal. Methods* **2014**, *6*, 1488–1500. [CrossRef]
15. Volpi, F.; Fiocco, G.; Gargano, M.; Albano, M.; Calvia, A.; Saviotti, F.; Delledonne, C.; Lee, C.; Rovetta, T.; Malagodi, M. Unveiling Materials and Origin of Reused Medieval Music Parchments by Portable XRF and ER-FTIR. *Microchem. J.* **2024**, *205*, 111224. [CrossRef]
16. López-Baldomero, A.B.; Buzzelli, M.; Moronta-Montero, F.; Martínez-Domingo, M.Á.; Valero, E.M. Ink Classification in Historical Documents Using Hyperspectral Imaging and Machine Learning Methods. *Spectrochim. Acta Part A Mol. Biomol. Spectrosc.* **2025**, *335*, 125916. [CrossRef]
17. Weller, A.; Van Velzen, B.; Koek, E. A Survey on the Use of Ultraviolet Induced Visible Luminescence in Paper Conservation. *Conserv. 360°* **2019**, *1*, 279–327.
18. Pronti, L.; Romani, M.; Lanteri, L.; Bizzarri, F.; Colantonio, C.; Pelosi, C.; Ruberto, C.; Castelli, L.; Mazzinghi, A.; Spizzichino, V. Non-Invasive Investigation of a 16th-Century Illuminated Scroll: Pigments, Fillers, and Metal-Based Decorations. *Minerals* **2025**, *15*, 1252. [CrossRef]
19. Picollo, M.; Cucci, C.; Casini, A.; Stefani, L. Hyper-Spectral Imaging Technique in the Cultural Heritage Field: New Possible Scenarios. *Sensors* **2020**, *20*, 2843. [CrossRef] [PubMed]
20. Aceto, M.; Arrais, A.; Marsano, F.; Agostino, A.; Fenoglio, G.; Idone, A.; Gulmini, M. A Diagnostic Study on Folium and Orchil Dyes with Non-Invasive and Micro-Destructive Methods. *Spectrochim. Acta A* **2015**, *142*, 159–168. [CrossRef]
21. Aceto, M.; Calà, E.; Agostino, A.; Fenoglio, G.; Gulmini, M.; Idone, A.; Porter, C.; Hofmann, C.; Rabitsch, S.; Denoël, C.; et al. Mythic Dyes or Mythic Colour? New Insight into the Use of Purple Dyes on Codices. *Spectrochim. Acta Part A Mol. Biomol. Spectrosc.* **2019**, *215*, 133–141. [CrossRef] [PubMed]
22. Vnouček, J.; Fiddyment, S.; Quandt, A.; Rabitsch, S.; Collins, M.; Hofmann, C. The Parchment of the Vienna Genesis: Characteristics and Manufacture. In *The Vienna Genesis*; Hofmann, C., Ed.; Böhlau Verlag: Vienna, Austria, 2020; pp. 35–70, ISBN 978-3-205-21057-3.
23. Bentivoglio-Ravasio, B. Un'introduzione al Codice. In *Il Libro D'ore Durazzo: Volume Di Commento*; De Marchi, A., Ed.; Franco Cosimo Panini: Modena, Italy, 2008; pp. 189–222, ISBN 978-88-248-0444-8.
24. Fornacelli, C.; Cucci, C.; Casini, A.; Aceto, M.; Picollo, M. Hyperspectral Imaging for the Colorimetric Characterization of Purple Manuscripts: Accuracy, Biases, and Diagnostic Potential. *Sensors* **2026**, *26*, 3358. [CrossRef] [PubMed]
25. Signoroni, A.; Conte, M.; Plutino, A.; Rizzi, A. Spatial–Spectral Evidence of Glare Influence on Hyperspectral Acquisitions. *Sensors* **2020**, *20*, 4374. [CrossRef] [PubMed]
26. Nivoloni, L. Scheda Codicologica. In *Il Libro D'ore Durazzo: Volume Di Commento*; De Marchi, A., Ed.; Franco Cosimo Panini: Modena, Italy, 2008; pp. 253–257, ISBN 978-88-248-0444-8.
27. Aceto, M.; Calà, E.; Gulino, F.; Gullo, F.; Labate, M.; Agostino, A.; Picollo, M. The Use of UV-Visible Diffuse Reflectance Spectrophotometry for a Fast, Preliminary Authentication of Gemstones. *Molecules* **2022**, *27*, 4716. [CrossRef] [PubMed]
28. Rabitsch, S.; Boesken Kanold, I.; Hofmann, C. Purple Dyeing of Parchment. In *The Vienna Genesis: Material Analysis and Conservation of a Late Antique Illuminated Manuscript on Purple Parchment*; Hofmann, C., Ed.; Böhlau Verlag: Vienna, Austria, 2020; pp. 71–101, ISBN 978-3-205-21057-3.
29. Pertica, A.; Casini, A.; Cucci, C.; Picollo, M.; Stefani, L.; Vervat, M. Reflectance Hyperspectral Imaging for Colorimetric and Spectroscopic Studies: The Analysis of an Impressionist Painting. *Color Cult. Sci.* **2023**, *15*, 75–82. [CrossRef]
30. Lorusso, S.; Natali, A.; Matteucci, C. Colorimetry Applied to the Field of Cultural Heritage: Examples of Study Cases. *Conserv. Sci. Cult. Herit.* **2007**, *7*, 187–220. [CrossRef] [PubMed]
31. Dolgin, B.; Bulatov, V.; Schechter, I. Non-Destructive Assessment of Parchment Deterioration by Optical Methods. *Anal. Bioanal. Chem.* **2007**, *388*, 1885–1896. [CrossRef] [PubMed]
32. Axelsson, K.M.; Larsen, R.; Sommer, D.V.P.; Melin, R. Degradation of Collagen in Parchment under the Influence of Heat-Induced Oxidation: Preliminary Study of Changes at Macroscopic, Microscopic, and Molecular Levels. *Stud. Conserv.* **2016**, *61*, 46–57. [CrossRef]
33. Kennedy, C.J.; Wess, T.J. The Structure of Collagen within Parchment—A Review. *Restaurator* **2003**, *24*, 61–80. [CrossRef]
34. Oderzo-Gabrieli, B. L'inventario Della Spezieria Di Pietro Fasolis e Il Commercio Dei Materiali per La Pittura Nei Documenti Piemontesi (1332-1453). *Boll. Della Soc. Stor. Pinerolese* **2013**, *30*, 7–53.
35. Oderzo-Gabrieli, B. L'inventario Della Spezieria Di Pietro Fasolis e Il Commercio Dei Materiali per La Pittura Nei Documenti Piemontesi (1332-1453). *Boll. Della Soc. Stor. Pinerolese* **2012**, *29*, 7–43.

36. Nash, S. 'Pour Couleurs et Autres Choses Prise de Lui . . .': The Supply, Acquisition, Cost and Employment of Painters' Materials at the Burgundian Court, c. 1375–1419. In *Trade in Artists' Materials: Markets and Commerce in Europe to 1700*; Kirby, J., Nash, S., Cannon, J., Eds.; Archetype Publications Ltd.: London, UK, 2010; pp. 97–182.
37. Kubersky-Piredda, S. The Market for Painters' Materials in Renaissance Florence. In *Trade in Artists' Materials: Markets and Commerce in Europe to 1700*; Kirby, J., Nash, S., Cannon, J., Eds.; Archetype Publications: London, UK, 2010; pp. 223–243.
38. DeLancey, J.A. Shipping Colour: Valute, Pigments, Trade and Francesco Di Marco Datini. In *Trade in Artists' Materials. Markets and Commerce in Europe to 1700*; Kirby, J., Nash, S., Cannon, J., Eds.; Archetype Publications Ltd.: London, UK, 2010; pp. 74–85, ISBN 978-1-904982-25-8.
39. Delamare, F. *Blue Pigments: 5000 Years of Art and Industry*; Archetype Publications: London, UK, 2013.
40. Kirby, J. Painting in a Wider World: Developments in the Trade in Painters' Materials. In *Proceedings of the Trading Paintings and Painters' Materials 1550–1800, Copenhagen, Denmark, 21–22 June 2018*; Christensen, H., Jager, A., Eds.; Archetype Publications Ltd.: London, UK, 2019; pp. 1–14.
41. De Laurentiis, E. Messale Del Cardinale Domenico Della Rovere. In *Manoscritti, Incunaboli e Ritagli Miniati*; Castronovo, S., Crivello, F., Marzo, A., Saroni, G., Eds.; L'Artistica Editrice: Savigliano, Italy, 2025; pp. 312–327, ISBN 978-88-7320-493-0.
42. Cortea, I.M.; Ratoiu, L.; Rădvan, R. Non-Destructive Investigation of a Late Panel Painting by Lucas Cranach the Elder. In *Lasers in the Conservation of Artworks XIII: Proceedings of the International Conference on Lasers in the Conservation of Artworks XIII (LACONA XIII), Florence, Italy, 12–16 September 2022*; Siano, S., Ciofini, D., Eds.; CRC Press: London, UK, 2023; pp. 22–30, ISBN 978-1-003-38687-2.
43. Lanterna, G.; Picollo, M.; Radicati, B. Le Indagini Scientifiche Non Invasive Sull'Evangelario. In *Il Tetravangelario Di Rabbula. Firenze, Biblioteca Medicea Laurenziana, Plut. 1.56. L'illustrazione Del Nuovo Testamento Nella Siria Del VI Secolo*; Edizioni di Storia e Letteratura: Roma, Italy, 2008; pp. 135–144.
44. Clark, R.J.H.; Gibbs, P.J. Identification of Lead (Ii) Sulfide and Pararealgar on a 13th Century Manuscript by Raman Microscopy. *Chem. Commun.* **1997**, *33*, 1003–1004. [CrossRef]
45. Knipe, P.; Eremin, K.; Walton, M.; Babini, A.; Rayner, G. Materials and Techniques of Islamic Manuscripts. *Herit. Sci.* **2018**, *6*, 55. [CrossRef]
46. Barners, S.; Tsang, J.S. Formation of Efflorescence and Soaps in a Group of 31-Year-Old Tempera Paints: A Baseline for Comparison. In *Tempera Painting 1800–1950*; Dietemann, P., Neugebauer, W., Ortner, E., Poggendorf, R., Reinkowski-Häfner, E., Stege, H., Eds.; Archetype Publications Ltd.: London, UK, 2019; pp. 191–194, ISBN 978-1-909492-59-2.
47. Kasyanenko, I.M.; Kramarenko, V.Y. The Effect of Pigment Volume Concentration on Film Formation and the Mechanical Properties of Coatings Based on Water-Dispersion Paint and Varnish Materials. *Mech. Compos Mater.* **2018**, *53*, 767–780. [CrossRef]
48. Baldomero, L.; Belén, A. Hyperspectral Image Processing for Material Identification in Historical Documents and Artworks. Doctoral Thesis, Universidad de Granada, Grenada, Spain, 2025.
49. Behmann, J.; Acebron, K.; Emin, D.; Bennertz, S.; Matsubara, S.; Thomas, S.; Bohnenkamp, D.; Kuska, M.T.; Jussila, J.; Salo, H.; et al. Specim IQ: Evaluation of a New, Miniaturized Handheld Hyperspectral Camera and Its Application for Plant Phenotyping and Disease Detection. *Sensors* **2018**, *18*, 441. [CrossRef] [PubMed]